*Fibers and Polymers* 2019, Vol.20, No.7, 1387-1395
DOI 10.1007/s12221-019-8524-9

ISSN 1229-9197 (print version)
ISSN 1875-0052 (electronic version)

# Preparation of Multi-Functional Polyester Fabrics with the Use of a New Organo-Clay Nanopigment in High Temperature/High Pressure Condition

**A. Almasian[1]*, M. Mirjalili[2], L. Maleknia[3,4], and M. Giahi[3,5]**

[1]*Nanotechnology Research Center, Islamic Azad University, South Tehran Branch, Tehran 1584743311, Iran*
[2]*Department of Textile, Yazd Branch, Islamic Azad University, Yazd 8916871967, Iran*
[3]*Nanotechnology Research Center, Islamic Azad University, South Tehran Branch, Tehran 1584743311, Iran*
[4]*Department of Biomedical Engineering, Islamic Azad University, South Tehran Branch, Tehran 1584743311, Iran*
[5]*Department of Chemistry, Lahijan Branch, Islamic Azad University, Lahijan 4416939515, Iran*
(Received June 19, 2018; Revised February 11, 2019; Accepted March 12, 2019)

**Abstract:** For the first time, the ability of dyeing the montmorillonite (Mt) mineral with reactive dye aiming to prepare a new nanopigment was investigated and the optimum conditions were determined. The prepared nanopigment was characterized by Fourier-transform infrared spectra (FTIR), transmission electron microscope (TEM), Brunauer-Emmett-Teller (BET), reflectance spectrophotometer (RS) and colorimetry analyses. The results showed that the dye molecules were attached to the hydroxyl groups of Mt plates through a covalent linkage. Also, the BET surface area values slightly increased after the dyeing process due to the separation of Mt plates and the reduction of particle size because of penetration of dye molecules among the plates. Colorimetry analysis revealed that the intercalation of dye molecules was depended on dye concentration and number of reactive sites on the Mt surface. The prepared nanopigment was used for dyeing the polyester fabric in high pressure and temperature conditions. The SEM, colorimetry, electromagnetic reflectance, flammability, and TGA tests were performed to investigate the properties of fabrics. Results indicated that intercalation of Mt nanopigment in the polyester fiber enhances the flame retardant, electromagnetic reflection and breathability of fabrics. Also, the optimum amount of nanopigment in the dyeing process was reported. It can be suggested that the prepared fabric can be a good candidate for utilizing in military and electronic aspects.

**Keywords:** Montmorillonite, Intercalation, Nanopigment, Electromagnetic reflection, Polyester dyeing

## Introduction

Polyethylene terephthalate (PET) fiber, which is a type of polyester fiber, have taken a major position in textiles because of their excellent physical properties, such as the tensile strength, crease recovery angle, and biological resistance. However, they show poor comfort properties because of their low moisture regain, which causes to accumulate static charge and soiling. PET fibers are mostly dyed by disperse dyes at high temperatures due to its hydrophobic, non-ionic nature and highly compact molecular structure [1]. It swells to a very small extent in the water bath. Hence, the access of the dye molecules into the fibers is very difficult. In this regard, dyeing process usually performs by a non-ionic dyestuff along with high temperature and/or pressure conditions [2,3]. In some cases, the use of carrier is regarded as a proper method for PET dyeing [4,5]. However, many of the carriers have disadvantages such as toxicity, unpleasant odor and environmental contamination [6]. In the last decade, many methods are employed to enhance the dye ability and comfort properties of polyester such as corona, plasma, ultraviolet irradiation, and $CO_2$ laser radiation [7-9]. Some of these methods often damage fibers and cause to increase the manufacturing costs [10].

A new emerging field in developing the novel pigments is nanopigment with application in coloring the polymer matrix as to obtain coatings, and various types of substrates such as wood, paper, latex, glass, metals and textiles. Nano pigments have high surface area, which results higher surface coverage, and high number of reflectance points, hence improved scattering.

Clay minerals are the most common inorganic materials on the earth's surface which are mostly used in various fields including nanocomposites, ceramics, paper coatings, pharmaceuticals, ion exchangers, separators, and catalysts. These minerals, which belong to phyllosilicate group, have excellent properties such as high adsorption capacity and cation exchange. Among the various types of layered clay (kaolin, montmorillonite, attapulgite, mica, bentonite and saponite), montmorillonite is attracted the researchers due to its great abundance, low cost, and particular properties. Also, montmorillonite can interact with organic molecules through electrostatic interactions, secondary bonding or covalent bonding [11].

The use of inorganic nanopigments and nanoparticles on the artificial and natural fabrics for different purposes has been considered due to their great abundance and low cost [12,13]. To do this, ex-situ application of these materials on textiles has been reported [14]. However, this method was cost-inefficient and need post fixation treatments [14]. In situ, sonochemical in-situ synthesis and microwave assisted synthesis were the other methods for this purpose [15-19]. It

*Corresponding author: arashalmasi@yahoo.com

is also reported that the nano $TiO_2$ can be used for dyeing of polyester fabric with disperse dye without carrier [20]. The application of nanoparticles to textile materials relies on development of new technology that should provide desired effects for materials with long-term durability and stability without use of highly toxic organic compounds.

The organically modified nanoclays, which can be classified as a nanopigment, have gained remarkable importance as nano additives because they can improve the polymer properties like mechanical strength, thermal stability and barrier properties [12]. Introducing the organically modified clay to the polymer matrix also reduces some drawbacks, including bleeding, low lightfastness, and low stability against oxygen, temperature, and UV radiation. The modification of clay is usually performed by cationic exchange process with an organic dye and with organic surfactants. Furthermore, nanopigments can be a good alternative for traditional pigments that contain heavy metal in their structure and are highly contaminant. Many attempts were performed on producing the nanopigments hybrid such as intercalation of rhodamine B and methylene blue in montmorillonite [21,22]. In another study, it was observed that samples of polystyrene colored with nanopigments have a significant improvement on the thermal and UV stability [23].

The reactive dyes are the most popular dyes for dyeing cotton due to their brightness of shade, flexible application procedures and good color fastness properties of the dyed products. It is known that reactive dyes react with hydroxyl groups of cellulose through a nucleophilic substitution or addition and form the covalent bonds under alkaline conditions [24]. Until now, all the performed studies on preparation of organically modified clay nanopigments were based on cation exchange and electrostatic interaction and there is no study on preparation of nanopigments with covalent linkage. A literature review showed that the clay minerals were not modified with reactive dyes aiming to prepare a nanopigment. In this study, firstly, the ability of dyeing the montmorillonite (hereafter; Mt) with reactive dyes was investigated. Secondly, aiming to preparation of a multi-functional fabric, the prepared nanopigment was intercalated to the polyester fibers by a dyeing machine in high pressure and temperature conditions and the changes in properties of colored fabric compared to untreated one were evaluated.

The dyeing machine used in this study was Daelim Starlet which is classified as laboratory dye machine. Many kinds of these dyeing machines are introduced by other manufacturers (Ahiba, Gavazzi, etc.). However, industrial types of these machines are existed and manufactured by many companies such as F&P PERFECT, Shaoyang Textile Machinery and JOGSON dye machine. The synthesized nanopigment and the introduced dyeing process can produce multi-functional yarns and fabrics in industrial scale.

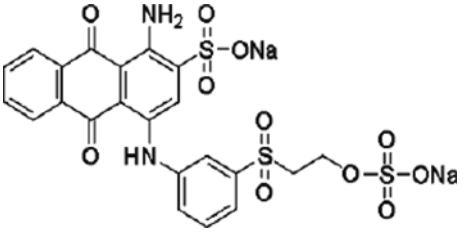

**Figure 1.** Molecular structure of the dye RB19.

## Experimental

### Materials

Polyester fabric was obtained from Yazd Baft Co. Nonionic detergent was provided by SDL Technologies for the scouring of the fabrics. The dispersing agent was Ekalin F from Sandoz Company (Holzkirchen, Germany) and benzoic acid from Sigma Aldrich were used as dispersing agent and carrier, respectively. Acetic acid from Merck, Germany was used for the pH adjust. The reactive dye, C.I. Reactive blue 19 (RB19), used for dyeing clay was supplied by Alvan Sabet (Iran) company (Figure 1). Nanoclay particles of montmorillonite supplied by Sigma Aldrich Co. were used in this research. It contains 98.99 percent montmorillonite and as stated by the manufacturer, its cation exchange capacity is estimated to be 48 meq/100 g, in the chemical composition. Sodium hydrosulfite ($Na_2S_2O_4$) and sodium hydroxide (NaOH) were purchased from Merck, Germany.

### Preparation of Mt Nanopigment

2 g of Mt was added to 100 m*l* deionized water and the mixture was sonicated for 25 min to reduce the particle sizes. The reactive dye with different concentrations (1, 3, 5, 7 and 9 %w/w) was also dissolved in deionized water and added to the colloidal dispersions at 40 °C. Then, the temperature was gradually raised to 85 °C over 20 min and it was held at that temperature for 1 h. The pH of the dyeing batch was adjusted to 8.5 by sodium hydroxide (0.1 M). Finally, the mixtures were centrifuged and washed 15 times by successive agitations/centrifugations with deionized water. The obtained nanopigments were dried at 60 °C for 12 h.

### Dyeing of Polyester Fabric with Nanopigment

Mixtures containing various amounts of nanopigment (0.5-5 % o.w.f.), 2 % o.w.f. acetic acid (pH 5.5) and 10 % o.w.f. dispersing agent were prepared. Then, the fabrics were added to the mixtures and they were placed in dyeing machine. The temperature, time and pressure were set as 100 °C, 90 min and 2.7 bar, respectively. The liquor to good ratio (L:G) was 50:1. After the dyeing process, the fabrics were washed in a batch containing 10 % o.w.f. NaOH and 10 % o.w.f. $Na_2S_2O_4$ at 70 °C for 30 min.

### Characterization

The FTIR spectra of nanopigments were examined by the FTIR spectroscopy (ThermoNicolet NEXUS 870 FTIR from Nicolet Instrument Corp., USA). The surface morphology and structure of fabrics and nanopigments were investigated using a scanning electron microscope (SEM, LEO1455VP, and ENGLAND) and TEM (Zeiss-EM10C-100 KV). Surface area measurement of the nanopigments was carried out using Brunauer-Emmett-Teller (BET) analyzer (Micromeritics Gemini III 2375, USA). The reflectance spectra of the samples and CIELAB color co-ordinates ($L^*$, $a^*$ and $b^*$) were calculated using a Gretagmacbeth COLOREYE 7000A spectrophotometer.

The electromagnetic reflection (EMR) and transmission (EMT) were calculated according to ASTM D 4935-99 using the following equation [25]:

$$EMR = \left|\frac{E_2}{E_1}\right|^2 \quad (1)$$

$$EMT = \left|\frac{E_0}{E_1}\right|^2 \quad (2)$$

where $E_0$, $E_1$, and $E_2$ are the electric field intensity transmitted through the fabrics, the electric field intensity of field source and the electric field intensity reflected from the fabrics, respectively. The plane-wave was generated using a HP 8103C shielding effectiveness tester. All parameters were measured in dB.

Flammability of the samples was evaluated according to ASTM D 635. To do this, five samples with dimensions of 10 cm×2 cm were used. The thermal degradation analysis (TGA) of the samples was performed on a Perkin Elmer thermoanalyser (Pyris diamond SII) under $N_2$ at a heating rate of 5 °C/min from room temperature to 576 °C.

The moisture regain was determined according to ASTM 2654-76 using the following equation:

$$\text{Moisture regain \%} = \frac{(W_1 - W_2)}{W_2} \times 100 \quad (3)$$

where $W_1$ is the weight (g) of the sample after saturation at the standard humidity and $W_2$ is the weight (g) of the dried sample.

## Results and Discussion

### Optimizing the Dyeing Process of Nanopigment

The optimization of dyeing process was performed by varying the concentration of dye in process. The colorimetric analysis was used to investigate the changes of the color of samples in CIELAB color space and the results are shown in Table 1. The $L^*$, $a^*$ and $b^*$ are the three axes of this space. The $L^*$ is the color coordinate which represents the lightness of the samples and can be measured independently of the color hue [26]. Any decreases in the lightness of the samples can be interpreted as more color absorption into the Mt. The $a^*$ stands for the horizontal red-green color axis. The $b^*$ represents the vertical yellow-blue axis [27].

**Table 1.** Color co-ordinates of untreated and colored Mt

| Axes | $L^*$ | $a^*$ | $b^*$ |
|---|---|---|---|
| Untreated Mt | 85.39 | 0.22 | 7.61 |
| Colored Mt (1 %) | 45.68 | 0.18 | -19.12 |
| Colored Mt (3 %) | 38.78 | 0.14 | -23.47 |
| Colored Mt (5 %) | 29.41 | 0.06 | -28.27 |
| Colored Mt (7 %) | 22.82 | 0.01 | -31.64 |
| Colored Mt (9 %) | 23.04 | 0.04 | -31.51 |

According to the Table, with increasing the dye concentration in the process the $L^*$ values decreased. Also, it can be seen that for the dye concentration of 7 and 9 % w/w, the $L^*$ values are nearly the same. It could be related to the existence of a certain amount of reactive sites on Mt for attaching the dye molecules. After filling these sites, a saturation point reached. With an increment in the dye concentration (1-7 %w/w), the amount of attached molecules to the Mt surface increased because of increasing the driving force of the concentration gradient [28,29]. Further increase in the dye concentration led to raise the $L^*$ value which could be due to the aggregation of dye molecules on the surface of Mt. On the other hand, b* value decreased with raising the dye concentration in the dyeing process. Also, it was found that there is no significant change among the $b^*$ values when the dye concentration ranges from 7 to 9 %w/w. The results indicated that the dye concentration of 7 %w/w is optimum and it was used for further studies.

The optimum amount of dye concentration was also confirmed by evaluating the reflectance curves of nanopigments (Figure 2). As can be seen, the reflectance values of untreated Mt are higher than colored Mt due to high refractive index of silica existing in the Mt nanoparticles [30]. With increasing the dye concentration in dyeing process the reflectance values decreased because of more intercalation of dye

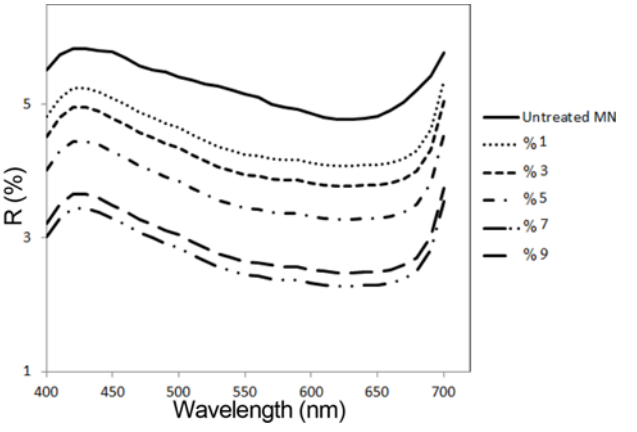


**Figure 2.** Reflectance curves of nanopigments.

molecules onto the Mt surface. The particle size and aggregation are the parameters affecting on reflectance behavior [31]. However, the reflectance of nanopigment colored with 9 %w/w reactive dye was higher than the sample colored with 7 %w/w dye. This can be due to the aggregation of dye molecules on the Mt surface. Similar result was reported by other researchers [32].

**FTIR Analysis of Nanopigment**

The FTIR spectra of untreated and colored Mt are shown in Figure 3. In the curve A, the bands at 400-550 $cm^{-1}$ generally correlated with Si-O-Si and O-Si-O bending modes [33]. Also, bands around 900-1100 $cm^{-1}$, are related to Si-O-Si anti-symmetric stretching of bridging oxygen within the tetrahedral [10]. The bending and stretching modes of absorbed water molecules in the interlayer of Mt mineral appeared at 1634 and 3434 $cm^{-1}$, respectively [34]. Also, the band at 695 $cm^{-1}$ is corresponded to aluminum-oxygen bonds of the lattice [35]. The peaks at 3651 and 3779 $cm^{-1}$ are related to the stretching vibration of structural hydroxyl group bonded to the aluminum and/or magnesium in Mt and the stretching modes of silanol Si(OH) groups, respectively [33]. Most of these peaks were seen in the colored sample but with lower intensity in comparison with untreated one. According to the curve B, the band at 3779 $cm^{-1}$, attributing to the stretching modes of silanol Si(OH) groups was disappeared. Also, the intensity of the bands at 1631 and 3439 $cm^{-1}$ were decreased. The appearance of the peak at 1105 $cm^{-1}$ can be attributed to the stretching mode of Si-O-C [36]. The asymmetric and symmetric vibrations of C-H bonds of dye molecules were appeared at 2924 and 2847 $cm^{-1}$, respectively. The band at 1574 $cm^{-1}$ was attributed to the bending vibration of secondary amine [37]. Also, the band appeared at 1381 $cm^{-1}$ is related to the vibration of S=O bond in $SO_2$ group [38]. The characteristic peaks of mineral compound were similar to curve A. Based on FTIR results, it can be concluded that dye molecules attach to the hydroxyl groups of Mt through the covalent linkage. The proposed mechanism for the reaction of Mt mineral with the reactive dye is presented at Figure 4.

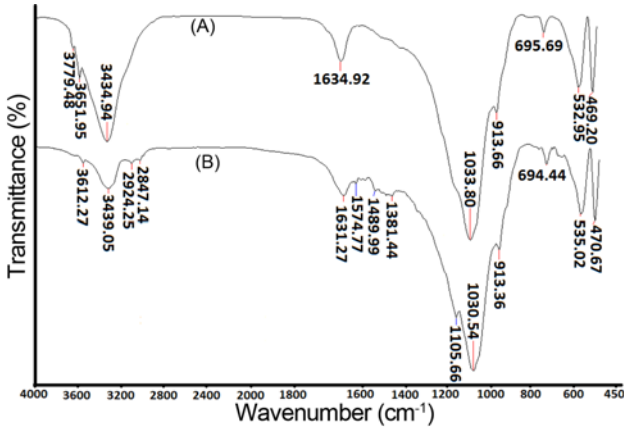


**Figure 3.** FTIR spectra of (A) Mt and (B) nanopigment (7 % w/w).

**TEM Analysis of Nanopigment**

Figure 4 showed the TEM images of untreated and colored Mt at different magnifications. As can be seen, the untreated Mt presented a layered and uniform structure (Figure 5(A)) with some aggregation of plates (Figure 5(B)). For the colored sample, the presence of dye molecule on the surface of plates was detected. The dye molecule appears black and the plate is light colored in the image. Also, the average thickness of the plates was 5 nm. It was found that the absorption of dye molecules at the edge of plates was higher than their surfaces (Figure 5(E)). According to the figures, the aggregation of plates was decreased after the dyeing process. This can be due to the presence of organic molecules on the surface of Mt plates. Furthermore, some dye molecules penetrate into the Mt layers, resulting to separation of Mt plates. These results were confirmed by the results of BET analysis. The BET surface area of untreated and colored Mt was measured as 96 and 103 $m^2/g$, respectively. Increasing the BET surface area value can be due to the decrease in the number of plate aggregations after the dyeing process. However, this increase was not significant. Wang et al. studied the absorption of basic dyes onto two types of montmorillonite [39]. They suggested that incorporation of organic molecule in the clay structure decreases the BET surface area value due to the surface screen and pore blocking effects. It can be concluded that the separation of plates was the major reason for increasing the surface area and it was conquered to the surface screen and pore blocking effects. Also, the attachment of dye molecules takes place by the hydroxyl groups of Mt thus, blocking of pores was not significant.

**Optimizing of Nanopigment Concentration in the Dyeing Process of Fabric**

The optimized concentration of nanopigment in dyeing

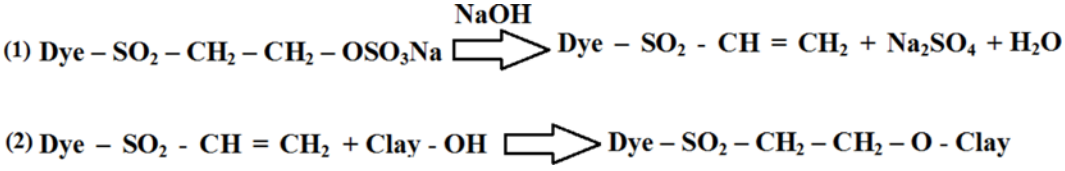


**Figure 4.** Proposed mechanism for the reaction of Mt mineral with the reactive dye.

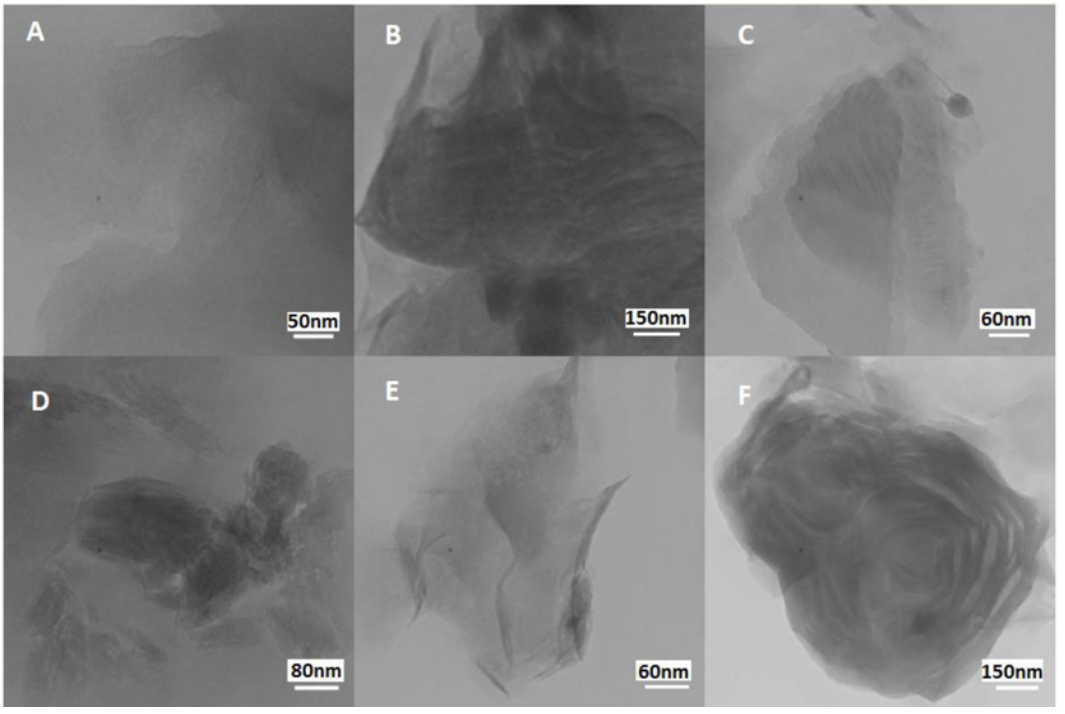


**Figure 5.** TEM images of (A, B, C) untreated Mt and (D, E, F) Mt nanopigment (7 % w/w).

**Table 2.** Color co-ordinates of untreated and colored fabrics

| Sample | L* | a* | b* |
|---|---|---|---|
| Untreated fabric | 95.5 | -0.4 | 0.1 |
| Colored fabric (0.5 %o.w.f.) | 70.22 | 0.07 | -14.12 |
| Colored fabric (2 %o.w.f.) | 65.49 | -0.12 | -18.47 |
| Colored fabric (3.5 %o.w.f.) | 59.51 | -0.13 | -21.27 |
| Colored fabric (5 %o.w.f.) | 58.62 | -0.02 | -25.64 |

**Table 3.** Moisture regain of untreated and colored fabrics

| Sample | Moisture regain (%) |
|---|---|
| Untreated fabric | 0.07 |
| Colored fabric (0.5 %o.w.f.) | 0.84 |
| Colored fabric (2 %o.w.f.) | 1.11 |
| Colored fabric (3.5 %o.w.f.) | 1.79 |
| Colored fabric (5 %o.w.f.) | 1.98 |

process of polyester fabric was determined by varying the nanopigment concentration in the range of 0.5-5 %o.w.f. To do this, colorimetric analysis in CIELAB color space was used and the results are shown in Table 2. From the Table 2, it was obvious that with raising the nanopigment concentration the $L^*$ values decreased. Decreasing the $L^*$ values could be due to more penetrations of nanopigment into the polyester fabric. Also, the $b^*$ value decreased with increasing the amount of nanopigment in dyeing process. However, the differences between the $L^*$ and $b^*$ values are negligible when the nanopigment concentration ranges from 3.5 to 5 %o.w.f. Since, the solid solution is the major mechanism for dyeing the polyester fabric with disperse dyes [40], it was concluded that a certain amount of disperse dyes could be incorporated into the polyester fibers. This conclusion could be used for dyeing the polyester fabrics with nanopigment because the dyeing mechanism was the same as disperse dyes. Further increase in the amount of nanopigment caused to agglomeration of dye molecules on the fiber surface. It was found that the concentration of 3.5 %w/w is the optimum.

The breathability of fabrics was investigated by determining the moisture regain of fabrics and the result is shown in Table 3. According to the table, the moisture regain value of the fabric colored with 0.5 %o.w.f. was much higher than untreated fabric due to the hydrophilic nature of Mt nanopigment which is capable to form hydrogen bonds with water molecules. Further increase in the concentration of nanopigment in dyeing process led to increase the moisture regain values.

## Electromagnetic Wave Reflectance and Horizontal Flammability Analyses

In this study, electromagnetic (EM) waves in the range of 5-8 GHz were used to evaluate the wave reflection property of colored fabrics. Generally, EM waves in the 1-10 GHz range are widely used in wireless communication tools and local area networks. Since, EM waves have negative effects

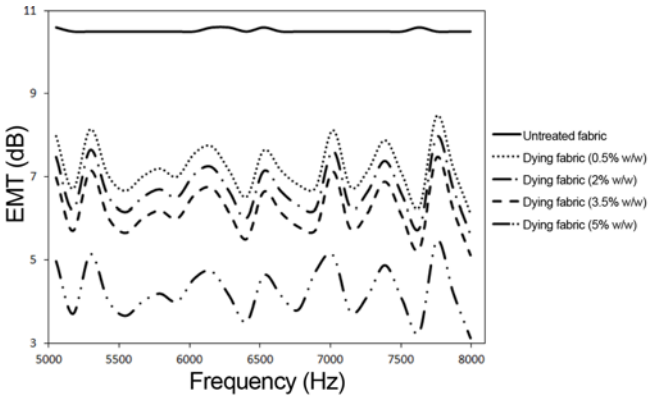


**Figure 6.** EMT curves for different fabrics.

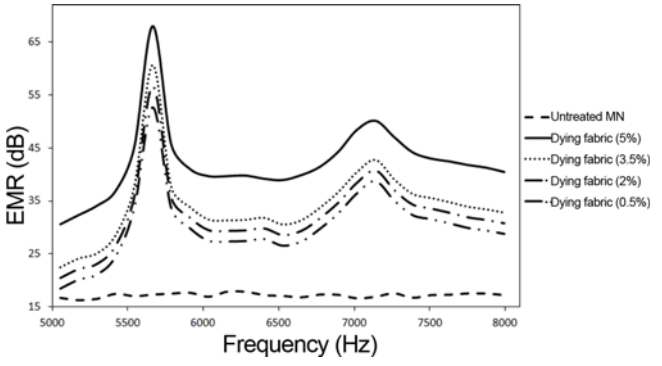


**Figure 7.** EMR curves for different fabrics.

on human health many EM-absorbing materials for shielding humans from EM fields are produced [41,42].

Figure 6 and 7 represented the electromagnetic wave transmission (EMT) and electromagnetic wave reflection (EMR) curves for untreated and the fabrics colored with different amounts of nanopigment, respectively. According to the Figure 5, the untreated fabric showed a fairly uniform structure with small fluctuation in transition in the range of 10 to 11 dB. For the colored fabric, a decrement in the transition was seen which is due to the incorporation of layered nanopigments into the polyester fiber. With increasing the nanopigment concentration, the amount of decrement in transition increased.

The reflection curve of untreated fabric showed a sinusoidal shape with fluctuation in the range of 17 to 19 dB. The reflection curves of colored fabrics presented two intense peaks at 5600 and 7100 MHz. As can be seen, the intensity of the peaks was increased when the amount of nanopigment increased in the dyeing process. An increment in the intensity of curves is related to the resonance due to geometry of matrix and clay characteristics [43]. However, the difference between the reflectance values of samples colored with the concentrations of 3.5 and 5 %o.w.f. was higher than the samples colored with the concentrations of 2 and 3.5 %o.w.f. This can be due to the agglomeration of nanopigments on the fiber surface.

The horizontal flammability analysis (HFA) was performed to evaluate the burning properties of the fabrics and the test results are shown in Table 4. According to the table, the burning length and time were decreased after the dyeing process. Increasing the concentration of nanopigment caused to more decrement of the burning length. The longer burning length and time indicates the greater the flammability [44]. Also, the intercalation of nanopigment in the fiber led to increasing the ignition time. It was found that the flammability of fabrics was enhanced significantly due to the presence of Mt nanopigments in the fiber matrix. The other researchers are previously stated that the flame-retardant property achieves by dispersing of the nano clay in the polymer matrix [10]. Also, the presence of clay mineral decreases the escaping rate of volatile decomposition products during the thermal analysis [45].

**SEM Images of Fabric**

The SEM and FE-SEM images of untreated and colored fabrics at different magnifications are shown in Figure 8. The untreated fabric was comprised of fibers with a uniform and smooth surface. Although, the smooth surface was nearly remained after the dyeing process, but some defects were seen on the fiber surface probably due to high pressure and temperature applied to the fabrics during the dyeing process. For the colored fabric with 5 %o.w.f. nanopigment, many aggregations were observed on the surface and touching point of fibers which is due to the agglomeration of nanopigment on the fiber surface. Aggregation of nanopigments on the surface of fibers decreases the tensile strength and force at break values of fabrics [46]. The SEM and FE-SEM results confirmed that the optimum concentration of nanopigment in dyeing process is 3.5 %o.w.f.

**Table 4.** Burning rate of untreated and colored fabrics

| Sample | Burned length (mm) | Burning time (s) | Ignition time (s) | Burning rate (mm/s) |
|---|---|---|---|---|
| Untreated fabric | 45 | 4.16 | 2.11 | 10.81 |
| Colored fabric (0.5 %o.w.f.) | 41 | 3.84 | 2.83 | 10.67 |
| Colored fabric (2 %o.w.f.) | 31 | 3.05 | 3.19 | 10.16 |
| Colored fabric (3.5 %o.w.f.) | 19 | 2.28 | 3.48 | 8.33 |
| Colored fabric (5 %o.w.f.) | 9.5 | 1.3 | 3.89 | 7.30 |

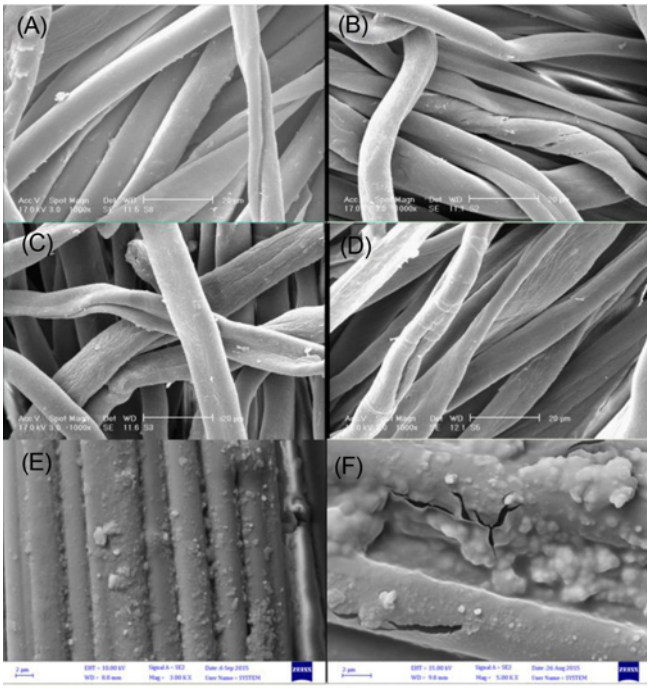


**Figure 8.** SEM image of (A) untreated polyester fabric, (B) colored fabric with 0.5 %o.w.f. nanopigment, (C) colored fabric with 2 %o.w.f. nanopigment, (D) colored fabric with 3.5 %o.w.f. nanopigment. FE-SEM image of (E) and (F) colored fabric with 5 %o.w.f. nanopigment.

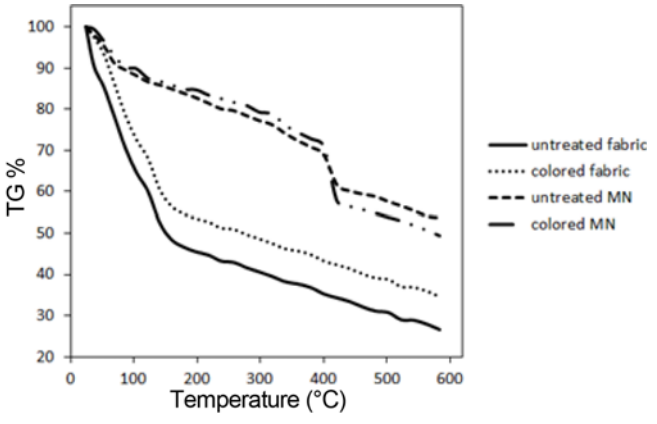


**Figure 9.** TGA curves for different fabrics.

## TGA Analysis

Thermal gravimetric analysis for untreated Mt, colored Mt, untreated fabric and colored fabric (3.5 %o.w.f.) was performed and the result is shown in Figure 9. The untreated M showed a high weight loss in the region of 30-150 °C. This is due to the removal of considerable amount of moisture adsorbed onto the clay surface [47]. The weight loss was continued in higher temperature because of the removal of chemisorbed water and dihydroxylation of silicate layer [48]. The dyeing of Mt caused to decrease the hydrophilicity of Mt resulted to lower weight loss in the temperature region of 30-150 °C. However, the amount of weight loss was higher than untreated Mt at higher temperatures due to the degradation of intercalated organic molecules on the Mt surface. The polyester fabric showed a significant weight loss in comparison with Mt and hybrid samples. The amount of weight loss was 60 % at the temperature of 450 °C. This value decreased to 39 % for colored fabric, indicating that the colored polyester is more thermally resistance than untreated one. The enhancement of the thermal properties is attributed to the heat insulation effect, the high heat resistance, and the mass transport barrier of nano Mt mineral [49].

## FTIR Analysis of Colored Fabric

The FTIR spectra of untreated polyester and colored fabric with 3.5 %w/w nanopigment are shown in Figure 10. In the polyester spectrum, the appeared bands at 795, 839 and 713 $cm^{-1}$ were attributed to C-C out of plane bending vibrations of the benzene rings. The bands at 3429 and 991 $cm^{-1}$ were related to intermolecular O-H groups bonded to C=O groups and O-H out of plane bending in terminal carboxylic groups in PET [50,51]. The stretching vibration of C-O-O and C-C was detected at 1098 and 1519 $cm^{-1}$, respectively. Esteric bonds for PET was characterized by the band at 1752 $cm^{-1}$, related to symmetric stretching of C=O groups. The weak bands observed at 3612 and 3575 $cm^{-1}$ can be attributed to stretching vibration of O-H of secondary alcohols. The bands appeared in the range of 2800-3000 $cm^{-1}$ and 1300-1500 $cm^{-1}$ were assigned to the stretching and bending vibrations of C-H in $CH_2$ and $CH_3$ groups, respectively [52]. After the intercalation of nanopigments in the PET matrix, the intensity of the bands at 3630, 3551 and 3340 $cm^{-1}$ was increased due to the presence of nanopigment into the fibers. Also, the band at 1752 $cm^{-1}$ was shifted to 1718 $cm^{-1}$ and the intensity of the band at 991 $cm^{-1}$ decreased. These changes may be attributed to the interactions between

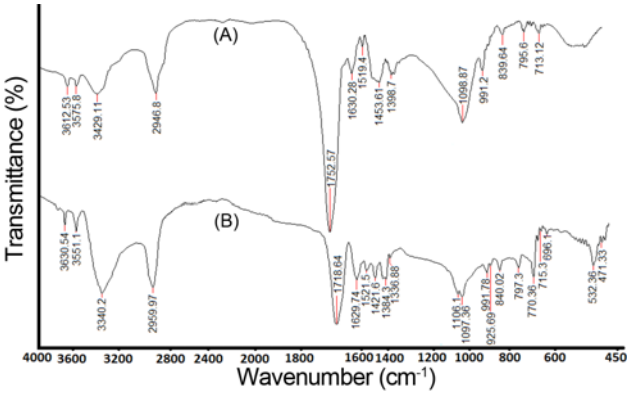


**Figure 10.** FTIR spectra of (A) untreated polyester fabric and (B) colored fabric with 3.5 %o.w.f. nanopigment.

intermolecular OH groups in terminals of carboxylic groups and OH groups of clay. Characteristic peaks related to nanopigment are almost the same as nanopigment spectrum (Figure 3 curve B). The FTIR results revealed that the hydrogen bonds can be formed between nanopigment and PET polymer after dyeing process.

In this study, the organoclay nanopigment was intercalated to the polyester fabric with a high temperature/high pressure dyeing machine. It is reported that the main mechanism for dyeing of polyester is solid solution [53,54] and intercalated dye molecules cannot release from the fibers in the usual condition. Dyeing is chemically called solid solution theory, as the disperse dyes do not dissolve but remain finely dispersed in water. The crystalline areas adsorb the dye at high temperature (130-140 $^{o}$C). All the used methods for polyester dyeing are based on the diffusion of dye molecules into the polymer matrix of fibers. In these methods, the interaction of dye molecules with polymer matrix does not play an important role because the dye molecules were forced to penetrate into the polymer matrix in high temperature and/or pressure conditions. High temperature makes the polymeric chains flexible and high pressure drives the dye molecules into the fibers. High temperature also increases the distance of polymeric chains and resulted to accelerate penetration of dye molecules. Dyeing process of polyester fabric with synthesized nanopigments is similar to dyeing process with disperse dyes.

## Conclusion

In this paper, a new organo-clay nanopigment was synthesized through the intercalation of a reactive dye into the montmorillonite mineral. The prepared nanopigment was characterized by various analyses. The results showed that a certain amount of dye molecules can be intercalated into the montmorillonite layer. Also, the reactive dye molecules attached to the surface of Mt plates by covalent linkages. The BET surface area values increased after dyeing process due to the decrease in the number of aggregation of montmorillonite plates resulted from the presence of organic molecules among the layers. The penetration of dye molecules among the plates was confirmed by TEM images. The prepared nanopigment was used for dyeing the polyester fabric. The colored fabric showed the flame retardant and electromagnetic reflection properties. Also, the moisture regain of fabrics increased after the intercalation of nanopigment into the fibers due to the hydrophilic nature of montmorillonite. The results showed that the hydrogen bonds were formed between nanopigment and PET polymer after dyeing process. It was concluded that the dyeing of polyester fabrics with the new nanopigments can prepare multi-functional textiles which can be used in military and electronic aspects.

## References


1. W. Ali, P. Sultana, M. Joshi, and S. Rajendran, *Adv. Mater. Res.-Switz.*, **64**, 399 (2016).
2. A. Walawska, B. Filipowska, and E. Rybicki, *Fibres Text. East. Eur.*, **11**, 41 (2003).
3. K. Kunttou, S. Hongyo, and S. Maeda, *Text. Res. J.*, **75**, 149 (2005).
4. O. Glenz, W. Beckmanann, and D. W. Wunde, *J. Soc. Dyers and Colourists*, **76**, 141 (1959).
5. F. J. Carrion Fite, *Text. Res. J.*, **65**, 362 (1995).
6. A. K. Choudhury, "Textile Preparation and Dyeing", Science Publishers, USA, 2006.
7. M. Montazer, J. Taheri, and T. Harifi, *J. Appl. Polym. Sci*., **124**, 342 (2012).
8. M. Parvinzadeh Gashti, I. Ebrahimi, and M. Pousti, *Curr. Appl. Phys.*, **15**, 1075 (2015).
9. S. Adeel, F.-U. Rehman, R. Hanif, M. Zuber, E.-U. Haq, and M. Munir, *Asian J. Chem*., **26**, 830 (2014).
10. M. Parvinzadeh Gashti, R. Rashidian, A. Almasian, and A. Badakhshan Zohouri, *Pigm. Resin. Technol.,* **42/3**, 175 (2013).
11. E. Ruiz-Hitzky, P. Aranda, and J. M. Serratosa in "Handbook of Layered Materials" (S. M. Auerbach, K. A. Carrado, and P. K. Dutta Eds.), pp.91-154, Marcel Dekker, New York, 2004.
12. S. Pavlidou and C. D. Papaspyrides, *Prog. Polym. Sci*., **33**, 1119 (2008).
13. H. Xu, X. Shi, Y. Lv, and Z. Mao, *Text. Res. J*., **83**, 321 (2013).
14. D. Wang, Y. Li, G. L. Pum, C. Wang, P. Wang, W. Zhang, and Q. Wang, *Appl. Catal., B*, **168-169**, 25 (2015).
15. F. Akhavan and M. Montazer, *Ultrason. Sonochem*., **21**, 681 (2013).
16. A. Behzadnia, M. Montazer, A. Rashidi, and M. Mahmoudi Rad, *Ultrason. Sonochem*., **21**, 1815 (2014).
17. I. Perelshtein, G. Applerot, N. Perkas, G. Guibert, S. Mikkhailov, and A. Gedanken, *Nanotechnology*, **19**, 245705 (2008).
18. V. Allahyarzadeh, M. Montazer, N. H. Nejad, and N. Samadi, *Polym. Biomed. Appl.*, **129**, 892 (2013).
19. L. Peng, R. Guo, J. Lan, S. Jiang, and S. Lin, *Appl. Surface Sci.,* **386**, 151 (2016).
20. T. Harifi and M. Montazer, *Dyes Pigment.*, **97**, 440 (2013).
21. M. I. Beltrán, V. Benavente, V. Marchante, H. Dema, and A. Marcilla, *Appl. Clay Sci.*, **97-98**, 43 (2014).
22. S. Raha, I. Ivanov, N. H. Quazi, and S. N. Bhattacharya, *Appl. Clay Sci*., **42**, 661 (2009).
23. J. Sivathasan, Masters Thesis, RMIT University, Melbourne, 2007.
24. N. S. E. Ahmed, *Dyes Pigment.*, **65**, 221 (2005).
25. G. Monti, L. Catarinucci, and L. Tarricone, *Microw Opt. Technol. Lett*., **52**, 1700 (2010).
26. H. Dave, L. Ledwani, and S. K. Nema, *Plasma Chem.*

*Plasma Process*, **36**, 599 (2016).
27. S. R. K. Velho, L. F. W. Brum, C. O. Petter, J. Henrique Z. dos Santos, S. Simuni, and W. Helmut Kappa, *Dyes Pigment.*, **136**, 248 (2017).
28. N. M. Mahmoodi, J. Abdi, and F. Najafi, *J. Colloid Interf. Sci.*, **400**, 88 (2013).
29. A. Almasian, F. Najafi, M. Mirjalili, M. Parvinzadeh Gashti, and Gh. Chizari Fard, *J. Taiwan Inst. Chem. E*, **67**, 306 (2016).
30. M. Parvinzadeh, S. Moradian, A. Rashidi, and M. E. Yazdanshenas, *Appl. Surf. Sci.*, **256**, 2792 (2010).
31. L. B. D. Paiva, A. R. Morales, and F. R. V. Díaz, *Appl. Clay Sci*., **42**, 8 (2008).
32. M. Parvinzadeh Gashti, A. Almasian, M. Parvinzadeh Gashti, *Sensor Actuat A-Phys*., **187**, 1 (2012).
33. E. M. A. Khalil, F. H. ElBatal, Y. M. Hamdy, H. M. Zidan, M. S. Aziz, and A. M. Abdelghany, *Physica B*, **405**, 1294 (2010).
34. A. Almasian, M. E. Olya, and N. M. Mahmoodi, *J. Taiwan Inst. Chem. E*, **49**, 119 (2015).
35. M. Parvinzadeh and Sh. Eslami, *Res. Chem. Intermed.*, **37**, 771 (2011).
36. C. A. Hacker, K. A. Anderson, L. J. Richter, and C. A. Richter, *Langmuir*, **21**, 882 (2005).
37. A. Almasian, N. M. Mahmoodi, and M. E. Olya, *J. Ind. Eng. Chem.,* **32**, 85 (2015).
38. V. Singha, A. Kumar Sharma, and R. Sanghi, *J. Hazard Mater*., **166**, 327 (2009).
39. C.-C. Wang, L.-C. Juang, T.-C. Hsu, C.-K. Lee, J.-F. Lee, and F.-C. Huang, *J. Colloid Interf. Sci.,* **273**, 80 (2004).
40. Z. Yi, F. Jihong, and C. Shuilin, *Color. Technol.*, **121**, 76 (2005).
41. J. D. Sudha, S. Sivakala, R. Prasanth, V. L. Reena, and P. Radhakrishnan Nair, *Compos. Sci. Technol.*, **69**, 358 (2009).
42. M. C. Golt, S. Yarlagadda, and J. W. Gillespie Jr., *J. Thermoplast. Compos. Mater*., **22**, 569 (2009).
43. M. Parvinzadeh Gashti and A. Almasian, *Compos. Part B-Eng.*, **43**, 3374 (2012).
44. M. Parvinzadeh Gashti, M. Y. Navid, and M. H. Rahimi, *J. Appl. Polym. Sci.*, **125**, 143 (2012).
45. J. Njuguna, K. Pielichowski, and S. Desai, *Polym. Adv. Technol*., **19**, 947 (2008).
46. D. W. Litchfield and D. G. Baird, *Polymer*, **49**, 5027 (2008).
47. M. Parvinzadeh Gashti and A. Almasian, *Compos. Part B-Eng*., **52**, 340 (2013).
48. M. Validi, S. Bazgir, A. Rashidi, and M. E. Yazdanshenas, *Ceram-Silikaty*, **56**, 152 (2012).
49. J. B. Dahiya and K. Kumar, *J. Sci. Ind. Res*., **68**, 548 (2009).
50. M. Parvinzadeh Gashti and A. Almasian, *Compos*. *Part-B Eng*., **45**, 282 (2013).
51. A. Almasian, M. L. Jalali, Gh. Chizari Fard, and L. Maleknia, *Chem. Eng. J.,* **326**, 1232 (2017).
52. A. Almasian, M. E. Olya, and N. M. Mahmoodi, *J. Taiwan Inst. Chem. Eng.*, **49**, 119 (2015).
53. S. R. Shukla, A. M. Harad, and L. S. Jawale, *Polym. Degrad. Stabil.,* **94**, 604 (2009).
54. D. Patterson and R. P. Sheldon, *Trans. Faraday Soc.*, **55**, 1254 (1959).